Journal of Non-Crystalline Solids 550 (2020) 120381

Contents lists available at ScienceDirect

Journal of Non-Crystalline Solids

journal homepage: www.elsevier.com/locate/jnoncrysol

On the presence of nanoscale heterogeneity in $Al_{70}Ni_{15}Co_{15}$ metallic glass under pressure

Achraf Atila[*,1,a], Meryem Kbirou[1,b], Said Ouaskit[b], Abdellatif Hasnaoui[c]

[a] Friedrich-Alexander-Universität Erlangen-Nürnberg, Materials Science and Engineering, Institute I, Martensstr. 5, Erlangen 91058, Germany
[b] Laboratoire de Physique de la Matière Condensée, Faculté des Sciences Ben M'sik, University Hassan II of Casablanca, B.P 7955, Av Driss El Harti, Sidi Othmane, Casablanca, Maroc
[c] LS3M Laboratory, Polydisciplinary Faculty of Khouribga, Sultan Moulay Slimane University of Beni Mellal, B.P. 145, Khouribga 25000, Morocco

ARTICLE INFO

Keywords:
Local atomic structure
Medium-range order
Heterogeneity
Correlation length
Glass transition

ABSTRACT

We used molecular dynamics simulations to investigate the dependence of the atomic-scale structure on the temperature and pressure conditions of $Al_{70}Ni_{15}Co_{15}$ metallic glass. The effect of pressure variations on the glass transition temperature was also studied, showing an increase with pressure. Moreover, radial distribution function, coordination number, and Voronoi tessellation analysis indicate that the applied pressure affects the local structure of glassy $Al_{70}Ni_{15}Co_{15}$. We used a local symmetry parameter to access the glass-forming ability of the metallic glasses cooled under different pressures. The glasses cooled under high-pressures showed a significant fraction of embedded crystalline structure, which was found to be surrounded by a region of mixed-like clusters playing the role of an interface between the crystalline region and the glassy region. The correlation length, as calculated from the full width at half maximum of the first sharp diffraction peak, indicated an increase of the medium-range order with the increase of pressure. The evolution of the heterogeneity with pressure was highlighted by the existence of nanoscale crystals (1 to 4 nm in size)embedded in the amorphous zone. Finally, we discuss the results by referring to the atomic potential energy and stress.

1. Introduction

The technological relevance of metallic glasses (MGs) has attracted the interests of physicists and materials scientists [1–7]. As amorphous materials, MGs are characterized by the lack of a long-range order, which made them even more fascinating. Due to their excellent mechanical properties (e,g,. high strength [8] and toughness [9]), MGs are potential candidates for many applications.

Glasses are obtained by quenching an equilibrated melt to a temperature below the glass transition temperature (T_g), with a cooling rate high enough to avoid the crystallization [10]. The glass transition temperature, is defined as the temperature range; bellow it, the supercooled liquid undergoes a dynamic slowdown [11]. The dynamic slowdown results from the inability of atoms to move and adapt in a configuration corresponding to that temperature, which in turn gives a configuration in a frozen non-equilibrium state. The glass transition temperature can be affected by many factors, among them, the cooling rate [12], the composition [13], the thermal and/ or the pressure history of the sample [14]. The structural change during the glass cooling process affects remarkably the physical properties of glasses. Hence, it is of great importance to decouple and understand how the structure changes in the cooling process under different thermodynamic conditions.

Molecular dynamics (MD) simulations, provide a powerful tool to study the behaviour of materials at an atomic-scale and has been successfully applied to studying the behaviour of materials under different thermodynamic conditions and for different systems such as silicate and bulk metallic glasses [12,13,15–24].

Recently, many papers investigated the effect of pressure (P) on the properties of MGs and liquids [25–30]. This is mainly due to the simple structure of metallic glasses and liquids (as compared to oxide glasses), which made them a model system for investigating the pressure effect on the properties of metallic liquids and glasses in order to understand the nature of the glass formation. Molecular dynamics simulations of CuNi alloy indicated that high pressure could favor glass formation, and different pressure values can lead to different glass transition temperatures [31]. The same tendency was shown on the monatomic zirconium showing that appropriate pressure can promote the formation

* Corresponding author.
E-mail address: achraf.atila@fau.de (A. Atila).
[1] These authors contributed equally to this work.

https://doi.org/10.1016/j.jnoncrysol.2020.120381
Received 6 July 2020; Received in revised form 12 August 2020; Accepted 18 August 2020

of amorphous phases [32]. Furthermore, it was found that compression of glasses results in higher Kasper polyhedrons, particularly ideal icosahedra fraction, which could enhance the glass-forming ability (GFA). Additionally, cooling under pressure could lead to a crystallization of the system. The crystallization behavior of metallic glass under pressure was reported by Wang et al. [33] they showed using MD simulations of NiAl alloys that the melts experience glass transition at P < 10 GPa while crystallizing at P ranging between 10–20 GPa. Miyazaki et al.[34] predicted using molecular dynamics simulations the presence of a pressure-induced rejuvenation in metallic glasses. This rejuvenation due to hydrostatic pressure increased the short- and medium-range order and leads to a higher-energy glassy state.

Al-based metallic glasses represent a particular interest due to their high strength and good ductility. Inoue et al. [35–37] succeeded in synthesizing binary AlY, AlLa, and AlCe Alloys and ternary AlCeM (M = Nb, Fe, Co, Ni or Cu) MG systems with good ductility, prepared by melt spinning. While, He et al. [38,39] reported an experimental study on the formation and stability of aluminum-based metallic glasses in AlFeGd alloys. Their good ductility, as well as excellent corrosion resistance behavior, makes them a promising candidate in engineering applications, structural as well as coating material [40]. Al-based metallic glasses can also be used as a depolluting agent for organic water contaminants when highly reactive elements such as Ca or Mg are included [41].

However, the GFA of Al-based metallic glasses is relatively low in comparison with other metallic glasses, which constitutes a limitation to applications. This disadvantage is because Al glassy alloys systems locate mostly away from their eutectic points where the liquidus temperature grows rapidly, resulting in a low reduced glass transition temperature T_{rg}. Due to their low glass-forming ability, which implies a high critical cooling rate ($\sim 10^6$ K/s), the synthesizes of Al-based metallic glasses are limited to the shapes of powders or thin ribbons, which restricts their practical applications. Although, recently, the formation of bulk Al-based MG was reported [42].

Otherwise, MGs appears to be macroscopically homogeneous, but their local properties may show significant heterogeneous signatures depending on their thermal/pressure history. These heterogeneities have been found to be responsible for several MGs physical and mechanical properties, such as plasticity [43] and the appearance of the Boson peak. Zhu et al. [44] suggested the presence of local structural heterogeneities in amorphous materials, characterized by either local static and/or dynamic properties. Zhang et al. [45] investigated the plastic deformation behavior of a nano-layered heterogeneous system (crystal Cu/amorphous Cu-Zr) and concluded to a deformation-induced devitrication. An et al. [46] identified the existance of a 1st order freezing transition from liquid to metastable heterogenous solid-like phase, when a supercooled liquid evolves isothermally below its melting temperature. This transition was found to be fundamentally linked to long-range elasticity.

Due to the presence of such heterogeneities, MGs are in a thermodynamically unstable state leading to a continuous change of their structure under relaxation or stress. Consequently, the local structural heterogeneities of an amorphous alloy can be altered or modied during a thermal and/ or mechanical treatment. An excellent review written by Qiao et al. [43] gives an extensive bibliography on this issue, highlighting the importance of such nanometer-scale structural features in the determination of mechanical behavior of the material. Controlling and understanding the nature of these heterogeneities would help in engineering MGs with desired mechanical/ thermodynamical properties. Kbirou et al. [19] studied the pressure ects on the local atomic structure of $Al_{70}Ni_{15}Co_{15}$ metallic glasses using values ranging up to 20 GPa. They showed that T_g increases while the degree of local five-fold symmetry decreases when the pressure increases. This decrease was accompanied by an increase of crystal-like clusters suggesting a possibility of a structural transition from the glass to a more crystal-like structure, but the amount of these last clusters was not high enough (less than 4%) to form crystalline regions. In the present work, we extend this work to higher pressure values to investigate the emergence of crystal-like regions embedded in a glass matrix forming a heterogeneous material. We performed MD simulations to study the pressure effects on the thermodynamic and structural properties of $Al_{70}Ni_{15}Co_{15}$ metallic alloy during the cooling process and in the glassy state. The local symmetry parameters were used to characterize the glass-forming ability of the system. Atomic stress and potential energy were also investigated to get some insight into the state of different atoms. The remainder of this paper is organized as follows, In Section 2, we briefly describe the procedure followed to obtain the glass as well as the interatomic potential used in this study. In Section 3, we present the results from our molecular dynamics simulations along with a discussion of the results. Concluding remarks are given in Section 4.

2. Computational details and methodology

To study the effect of the pressure on the thermodynamics and structural properties of $Al_{70}Ni_{15}Co_{15}$ metallic glass, a pressure ranging from 0 70 GPa was simulated by molecular dynamics simulations using the LAMMPS code [47]. Initially, 32,000 atoms were placed randomly in an FCC structure while ensuring the atomic composition of the studied system ($Al_{70}Ni_{15}Co_{15}$). An initial mean velocity corresponding to 300 K was attributed to the system following the Maxwell-Boltzmann distribution. The equations of motion were solved using the velocity-Verlet algorithm as implemented in LAMMPS with a timestep of 1 fs. Periodic boundary conditions were applied in all directions to avoid edge effect. The system was heated from 300 K to 2500 K using a heating rate of 10 K/ps and zero pressure. Keeping the temperature fixed at 2500 K, the pressure was increased gradually over a period of 1 ns from 0 GPa to the desired pressure. The system was held at the final pressure for 100 ps in NPT (constant number of particles N, pressure P, and temperature T). Then the liquid was cooled under pressure from 2500 K to 300 K using a cooling rate of 1 K/ps. The obtained glass was equilibrated at 300 K and using the same pressure for 500 ps in NPT. Finally, a 100 ps simulation in the NVT (constant number of particles N, volume V, and temperature T) ensemble was performed for statistical averaging. Nosé-Hoover thermostat and barostat were used to control temperature and pressure. It is worth stressing that the cooling rate used in this study is higher than the experimental counterpart, which is due to the limited time scales accessible by molecular dynamics.

The interaction between the system components are described using the Embedded-Atom Method (EAM) potential [48] where the total energy E_i of an atom is given by:

$$E_i = F_\alpha\left(\sum_{j\neq i}\rho_\beta(r_{ij})\right) + \frac{1}{2}\sum_{j\neq i}\phi_{\alpha\beta}(r_{ij}) \quad (1)$$

where F is the embedding energy which is a function of the atomic electron density ρ, ϕ describe pair potential interaction, and α and β are the element types of atoms i and j where r_{ij} is the interatomic distance. We adopted in this study the potential developed by Pun et al. [49] which reproduces successfully the martensitic phase transformation in ferromagnetic shape memory alloys of the NiAlCo system [49]. This potential was also used to simulate AlNiCo alloys and metallic glasses [19,20,50,51]. Moreover, this potential was successfully used for modeling metallic glasses [19,52]. It was used for investigating the local structural arrangement of the amorphous alloy system $Ni_{50}Al_{45}Co_5$ [52] subjected to uniaxial tensile deformation. The effect of flaw shape and size on the fracture toughness and the competition between brittle and ductile fracture in the $Al_{70}Ni_{15}Co_{15}$ MG were also evaluated through tensile deformation by using this potential. The interesting findings in these theoretical research provide some evidence of the validity of our theoretical findings and make the conclusions drawn from our simulations using this potential stronger.

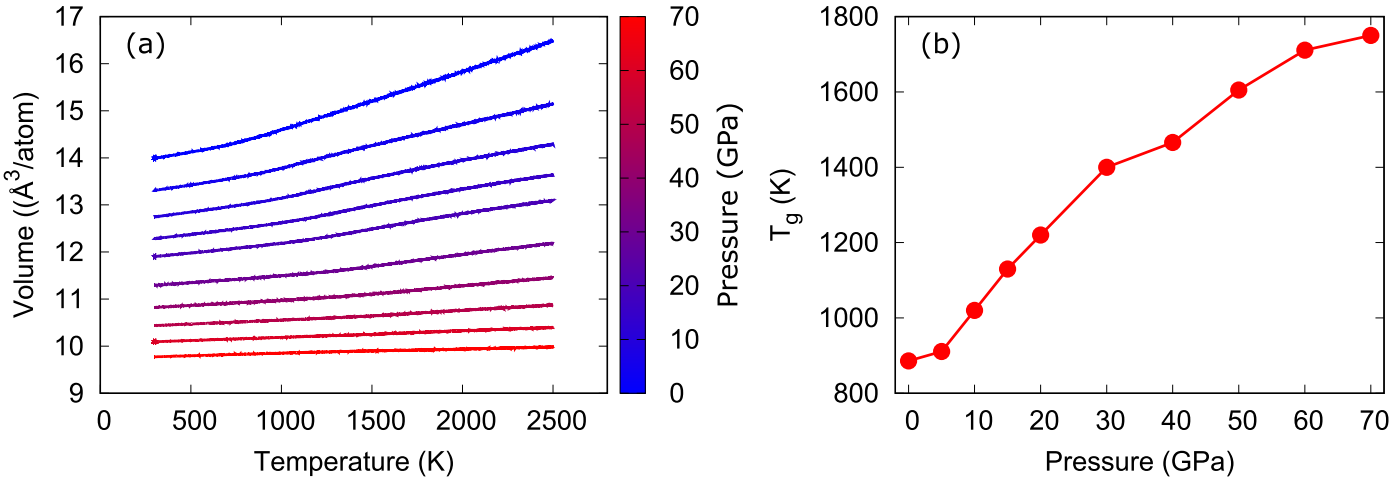

Fig. 1. (a) The variation of the volume as a function of the temperature for pressures ranging from 0 to 70 GPa. (b) Glass transition temperature as a function of pressure in the simulated $Al_{70}Ni_{15}Co_{15}$. The glass transition temperature values were obtained from the slope break of the low and high-temperature variation of the volume as a function of temperature. Lines are guide for the eyes.

3. Results and discussion

3.1. Glass transition temperature

The glass transition temperature T_g is defined as the temperature below which the supercooled liquid undergoes a dynamical arrest and therefore shows a solid-like behavior as the physical properties of the supercooled liquid change to those of a glassy state presenting rigidity and elasticity [11]. The glass transition temperature could be found by plotting the variation of some thermodynamic, chemical, or physical properties of the material such as volume, total energy, or enthalpy with temperature [12,13] or using some mechanical properties such as fracture toughness or elastic moduli [53,54]. The glass transition temperature is then obtained from the slope break between high- and low-temperature variations of that property versus temperature.

The values reported here are those obtained using the volume as a function of the temperature V(T). Fig. 1(a) depicts this variation during the cooling process and under different pressure values (P = 0, 5, 10, 15, 20, 30, 40, 50, 60, and 70 GPa). For all pressures, it can be seen that the volume decreases with decreasing temperature. The liquidglass transition is generally manifested by a change in the slope of V(T). The decrease of volume under higher pressure could cause shorter atomic diffusion distance. By extrapolating and intersecting two linear parts in the V(T) curve, T_g of the rapidly solidified metallic $Al_{70}Ni_{15}Co_{15}$ under the applied pressures is plotted versus the pressure as illustrated in Fig. 1(b). It is visible that T_g increases with increasing pressure in the studied range of pressures. This is consistent with the experimental observations of ZrTiCuNiBe system reported by Samwer et al. [55]. Thus, the higher the pressure, the higher the value of T_g. The increase of the glass transition temperature could be due to the fact that atoms at high pressure have less freedom to move toward lower energy basin in the energy landscape. However, when the pressure is applied during the cooling of a liquid, the interatomic distances tend to be reduced and thus having smaller clusters resulting in a much higher density. Therefore, the increase of T_g could be attributed to the decrease in the mobility of particles [56,57].

3.2. Structural analysis

3.2.1. Radial distribution function and structure factor

To investigate the atomic structure of the amorphous alloys obtained at different pressures, we first implemented the analysis of radial distribution function (RDF) and short-range structural order. Fig. 2(a–g) plot the total[2] and partial RDFs of $Al_{70}Ni_{15}Co_{15}$ glassy alloy at ten different pressure, which exhibits the following features:

- With increasing of the pressure, we note a shift towards lower r for all the peaks of the calculated RDFs. This implies that high pressure induces a decrease in the atomic nearest neighbor distance, which is generally employed to scale the size of the atom cluster in the liquids and glasses, to be decreased or transformed into another cluster type to accommodate this change. This is in agreement with the study of Wang et al. [33], which reported that an increase in pressure alters the atomic nearest neighbor distance, suggesting that the nearest neighbor distance between atoms is sensitive to the applied pressure.
- The intensity of the first peak of all RDFs, except that of the total and Al—Co ones, decreases with the increase of pressure. In fact, the total RDF originates from a superposition of the partial RDF functions of all pairs in which their contribution is proportional to the frequency of occurrence of different types of atomic pairs (Al—Al, Al—Co, Al—Ni Co—Co, Co—Ni, and Ni—Ni) in the structure of the MG. The fact that the increase in the intensity of the first peak is attributed to the total PDF and Al—Co indicates that there is a short-range order corresponding to Al—Co.
- Beyond the rst peak, the splitting in the second peak of the partial RDFs becomes more pronounced as the pressure increases. However, a shoulder develops on the second peak of Co—Ni PDF, which could be attributed to structural changes.

Fig. 3 (a) shows the total structure factor S(q) of the $Al_{70}Ni_{15}Co_{15}$ glassy state obtained by cooling under different pressures. It can be seen that all peaks shift towards high q values with increasing pressure, and their intensity increases with the pressure. In contrast to the RDF, the structure factor give some insight into the correlations at larger distances. The first sharp diffraction peak (FSDP) indicates the correlation at the medium-range structure of glasses [58–60]. The full width at half maximum (FWHM) of the FSDP is correlated to a medium-range correlation or coherence length L defined as $L = \frac{7.7}{FWHM}$ [58], to capture the correlation distance at the medium-range. In polycrystalline materials, the correlation length is related to the average size of the microcrystals based on the Scherrer equation [61]. While in amorphous solids, the correlation length is suggested to be representative of the average size of the rigid clusters in the atomic network [62,63]. As said before, the

[2] See supplementary materials Fig. 2 for a zoomed-in on the first and second peaks of the total RDFs.

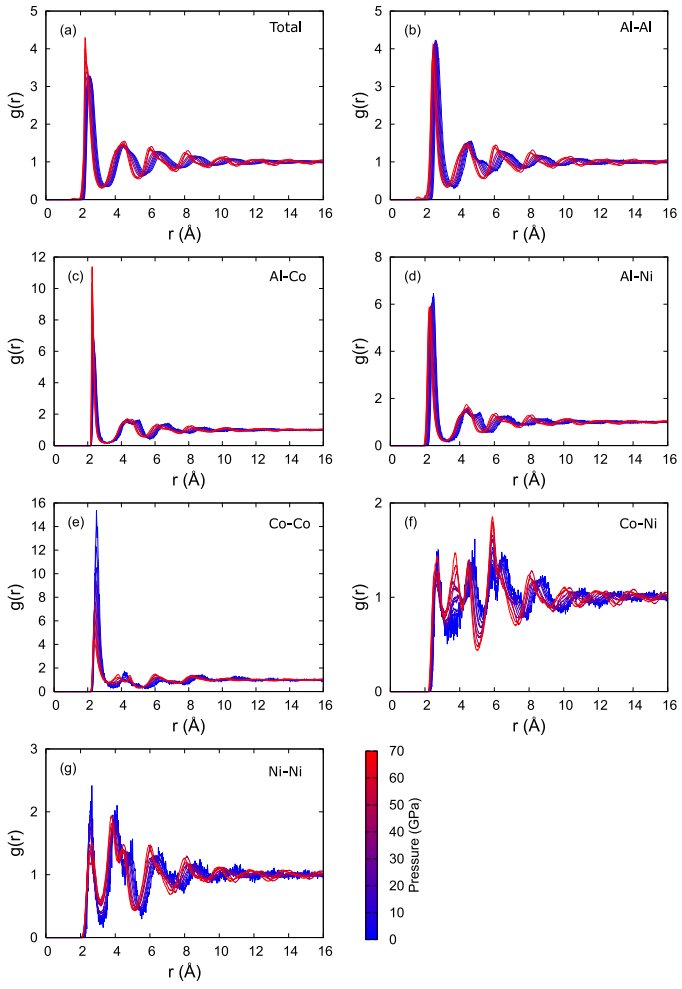

Fig. 2. Radial distribution functions at 300 K and for different pressure values. (a) Total RDF, (b) Al—Al, (c) Al—Co, (d) Al—Ni, (e) Co—Co, (f) Co—Ni, and (g) Ni—Ni, respectively.

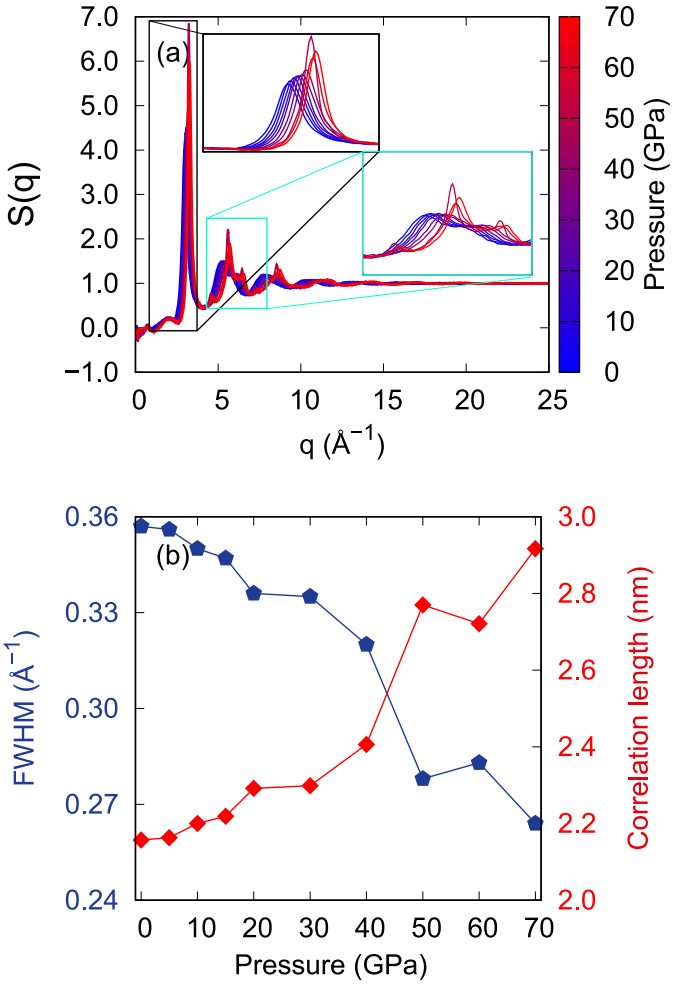

Fig. 3. (a) Total structure factor at 300 K for different pressure values. (b) The full width at half maximum of the total structure factor as a function of the pressure (left *y*-axis) and the corresponding correlation length (right *y*-axis) as function of the pressure.

FSDP becomes sharper with an increase in its intensity with the increase in the cooling pressure. This suggests that the correlation length in the medium-range order increases upon increasing the cooling pressure.

Fig. 3 (b) shows the full width at half maximum (FWHM) of the first sharp diffraction peak (FSDP) and the correlation length as a function of pressure. The FWHM of the $Al_{70}Ni_{15}Co_{15}$ glassy samples was obtained by fitting the first sharp peak with a Gaussian function. We observe that, with increasing of the cooling pressure, the FWHM decreases, and the correlation length increases, which suggests an increase in the degree of order within the medium-range structure of the glass.

3.2.2. Coordination number

To understand the relationship between atomic arrangements and high pressure in metallic glasses, the atomic order and detailed geometric information of the $Al_{70}Ni_{15}Co_{15}$ MG at different pressure will be investigated. The coordination number is used in structural studies to provide a statistical description of the nearest neighbor atomic environment in liquid and amorphous systems. The partial CN (CN_{ij}) is determined by integrating the curve of partial RDF up to its first minimum. The variation of the partial coordination numbers as a function of pressure in the $Al_{70}Ni_{15}Co_{15}$ alloy is shown in Fig. 4. According to Fig. 4(a), one can see that the values of $CN_{Al---Al}$ are significantly higher than those of other pairs. Upon increasing the pressure, it changes from 9.7 to 11, exhibiting an increasing trend. This is due to the fact that Al atoms have a higher fraction of the total composition. In the same context, the partial CN, such as $CN_{Ni---Ni}$, $CN_{Al---Ni}$, $CN_{Al---Co}$, and $CN_{Co---Ni}$ increase slightly with increasing pressure. Although the analysis shows that, an obvious decreasing trend of $CN_{Co---Co}$ with increasing pressure. It is known that the changes in CN under high pressure are associated with the modification of the atomic configuration of the metallic glass. Apparently, there exists a change in the variation tendencies of CN versus pressure, which reveals that the local ordering of the studied $Al_{70}Ni_{15}Co_{15}$ metallic glass increases due to a closer packing of the atoms in local ordering units under higher pressure. In other words, a reconstruction of the atomic configuration with further increasing pressure makes it possible to obtain a more ordered glassy structure.

3.2.3. Voronoi tessellation analysis and symmetry

In order to reveal the local atomic structure of the obtained amorphous systems, the Voronoi polyhedral analysis method has been chosen to provide the topological structural change of clusters under pressure. In this technique, the Voronoi cell is considered as the minimum volume convex cell surrounded by the vertical bisected planes between the central atom and the nearest neighbor atoms, which is also called a Voronoi polyhedron (VP) [64–66]. Each of these VPs is characterized by four Voronoi indices (n_3, n_4, n_5, n_6) where n_i represents the number of i-edged faces around the central atom. The Voronoi Polyhedral (VP) types have been divided into three types: icosahedral-like clusters (including $< 0,0,12,x >$, $< 0,1,10,x >$ *S*, $< 0,2,8,x >$), mixed clusters (including $< 0,3,6,x >$, $< 0,3,7,x >$)

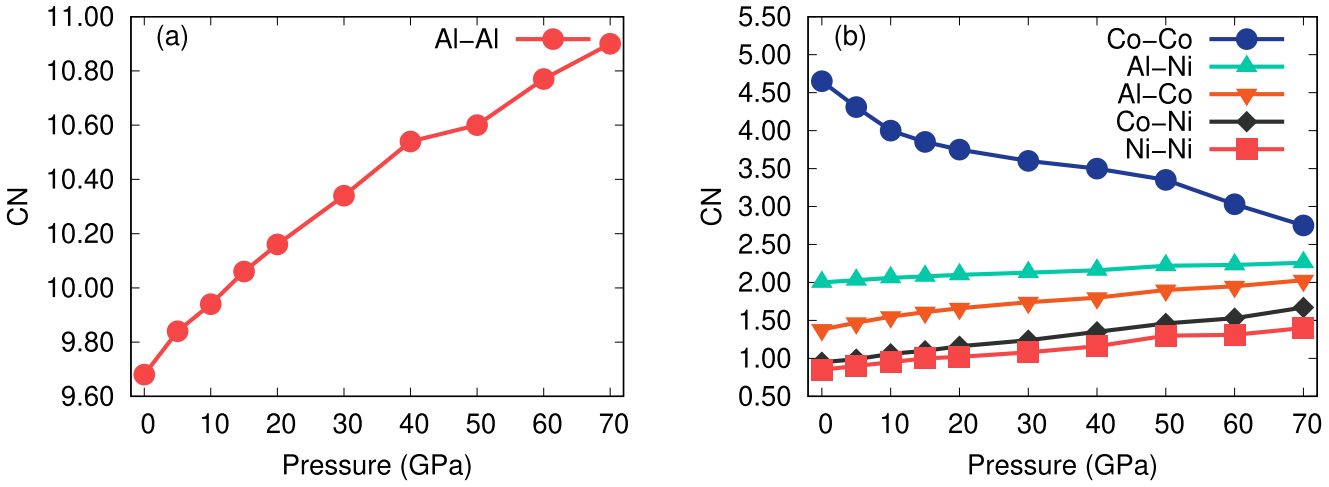

Fig. 4. Averaged coordination number as a function of the pressure of (a) Al—Al pair and (b) Co—Co, Al—Ni, Al—Co, Co—Ni, and Ni—Ni pairs at 300 K. Lines are guide for the eyes.

and crystal-like clusters (including all $< 0, 4, 4, x >$) where x is typically a number between 0 and 6 [67,68]. In this context, the pressure dependence of Voronoi cells (VCs), including the icosahedral-like, mixed-like, and crystal-like, were analyzed during the cooling process. The number of icosahedral-like clusters increases initially with decreasing temperature. At a pressure below 40 GPa, the number of the icosahedral-like clusters is almost the same during the quenching process and then decreases with increasing pressure. The same behavior has been observed for the crystal-like clusters, with the exception that the number of these clusters is firstly reduced with decreasing temperature.

The observed increase of the crystal-like clusters upon increasing pressure is due to the appearance of some crystalline regions which are randomly distributed in the amorphous matrix. This reveals that high pressure can promote the formation of crystal-like regions rather than glassy-like ones in the metallic rapidly solidified solids. This confirms the observations of CN, which indicates that higher pressure induces more order into the glassy structure. The mixed-like clusters tend to decrease during the rapid cooling; however, with increasing pressure, this decrease remains slightly remarkable. The configurations of $Al_{70}Ni_{15}Co_{15}$ alloy obtained at 300 K at four different pressures are presented in Fig. 5, which shows that the increase in pressure implies a significant increase in the bcc population. In fact, the CNA analysis showed that the percentage of bcc atom is 1.2% for 40 GPa, 14.6% for 50 GPa, 7.8% for 60 GPa, and 12.5% for 70 GPa, while it is lower than 1.2% for all other samples. Moreover, when a significant fraction of BCC atoms is found in the structure its composition is relatively the same as the base system ($Al_{70}Ni_{15}Co_{15}$). In general, the application of the pressure upon cooling leads to considerable changes in the structure, including the formation and the growth of crystal-like clusters. The size of these formed clusters in this alloy is influenced by the applied pressure.

The structure of $Al_{70}Ni_{15}Co_{15}$ obtained from MD simulations allows us to directly access to the nearest neighbor CN and other atomic packing details of the MG. The local atomic configuration and the geometry of the coordinated polyhedra in our system under different pressures have been examined using the Voronoi tessellation analysis. It is interesting to note that i-edged polygons in a Voronoi polyhedron can help to provide structural information about the atomic packing details and local atomic symmetry of the central atom and its surrounding nearest neighbors [69,70]. Therefore, four types of polygons, triangles, tetragons, pentagons, and hexagons represented respectively by the 3-, 4-, 5- and 6-fold symmetries [69,70] can characterize each polyhedron. The average degree of k-fold local symmetry can be defined based on the Voronoi analysis as follows:

$$W_k = \sum (f_i^k \times P_i) \quad (2)$$

where P_i is the fraction of polyhedron of type i and f_i^k represents the fraction of k-edged polygons in i-type VP and can be expressed as $f_i^k = \frac{n_i^k}{\sum_{k=3,4,5,6} n_i^k}$. We note that n_i^k denotes the number of edges in Voronoi polyhedron i. To reveal the local atomic symmetry change induced by compressive pressure, we calculated W_4,W_5,W_6, and W existing in the structure obtained during the quenching process from 2500 K to 300 K, under each pressure. The results of the changes are summarized in Fig. 6, which shows that we can specify three regimes. At low pressures (ranging from 0 to 30 GPa), when the temperature is lowered from 2500 K to 300 K, W_4 and W_6 first decrease sharply and begin to saturate at low temperatures where it can be said that a certain equilibrium between the different structural units is established. For intermediate pressures (35 to 40 GPa), an equilibrium occurs, preferably at higher temperatures, and we see that the curves exhibit a plateau-type behavior. However, at higher pressures ($>$ 40 GPa), W4 and W_6 show a different behavior where we initially observed a slight decrease when the temperature dropped to around 1700 K and a very abrupt increase followed by a plateau. On the other hand, we observed that W_5 exhibited a temperature-dependent behavior opposite to that of W_4 and W_6 as expected because these quantities are complementary. The behavior found at smaller pressures is consistent with computer simulations studies that have been performed for some MGs. It was reported that the evolution of pentagons with temperature is totally different from that of other type polygons (triangles, tetragons, and hexagons) [69,70].

At the short-range order (SRO), the icosahedral arrangement of atoms is generally accepted as the key structural feature in MGs [70–75]. The five-fold symmetry of these clusters is believed to arrest the MG dynamic below the glass transition temperature. From a geometric viewpoint, icosahedral clusters with fivefold symmetry are preferred SRO units in MGs due to their efficient packing [76–79]. However, these units cannot fill a 3D space due to their five-fold rotational symmetry, which is not compatible with long-range translational symmetry [80]. To accommodate this incompatibility in the 3D geometrical space, distorted icosahedra with partial fcc symmetry can pack together with perfect icosahedra in 3D space by arranging in specific modes of connectivity [81]. In an investigation of the short and medium-range orders in Co_3Al metallic glass using MD simulations, it was found that the first and second sub-peaks in the (RDF) corresponds to two icosahedral clusters, $< 0, 0, 12, 0 >$ and $< 0, 1, 10, 2 >$, respectively and their connectivity [20]. In binary Al—Co at 0 GPa, icosahedral-like and mixed-like structures are the most dominant, while

crystal-like clusters have been found to be rare [18].

On the other hand, in order to get insight into the structural details of the local atomic symmetry under pressure, we have proposed a structural parameter W based on the 4-, 5- and 6-fold symmetries. We simply define W as the ratio of the degree of 5-fold symmetry to the degree of the 4- and 6-fold symmetry, it is determined as:

$$W = \frac{W_5}{W_4 + W_6} \tag{3}$$

This parameter could help to quantify the local atomic symmetry and be a structural indicator to investigate structural atomic configuration in metallic glasses. The same behavior observed for W_5 is observed for W, with the exception that the values of W are a little higher than that of W_5. According to our results, there are two key aspects of local atomic symmetry change induced by the pressure in the investigated formation of $Al_{70}Ni_{15}Co_{15}$ glass. Firstly, if we restrict ourselves to the temperature-dependent of local atomic symmetry, we would confirm that the local five-fold symmetry plays a critical role in glass formation and can be regarded as one of the important geometrical features of amorphous structure. Secondly, the pressure prevents the formation of local five-fold symmetry and implies the competition and transformation between local five-fold symmetry and local, translational symmetry in local structures during glass formation since the 4- and 6-fold symmetry are reflecting the local, translational symmetry [82]. In the same context, Fig. 7(a) shows a slice of the atomic structure of a sample prepared using a pressure of 60 GPa, analyzed by the adaptive common neighbors analysis as used in OVITO [83], while Fig. 7(b) presents the same atomic slice colored according to the Voronoi index n_5 mapped from the blue for $n_5 = 0$ to red for $n_5 = 7$. The values of n_5 were Coarse-grained by averaging over neighbors in a 5Å -radius sphere. Note also that white color would correspond to intermediate values of $n_5 = 3$ or 4. As indicated in Fig. 7 (b) the crystalline region in the structure shows a very low Voronoi index n_5 (crystal-like clusters) highlighted as the region delimited by the yellow circle, surrounded by a region mixed between the amorphous and crystalline phases (mixed-like) as indicated by the black dashed circle, and the high values of n_5 indicates the glass structure which has higher values of icosahedral-like clusters. The mixed-like region is like an interface between the crystalline region and the amorphous region (See supplementary materials Fig. 3 for

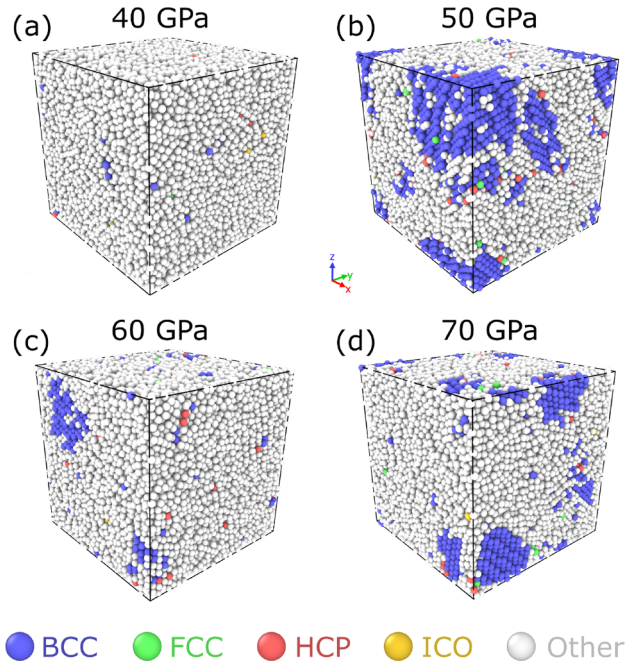

Fig. 5. Configuration of $Al_{70}Ni_{15}Co_{15}$ alloy obtained at 300 K for four selected Pressures (a) 40 GPa, (b) 50 GPa, (c) 60 GPa, and (d) 70 GPa.

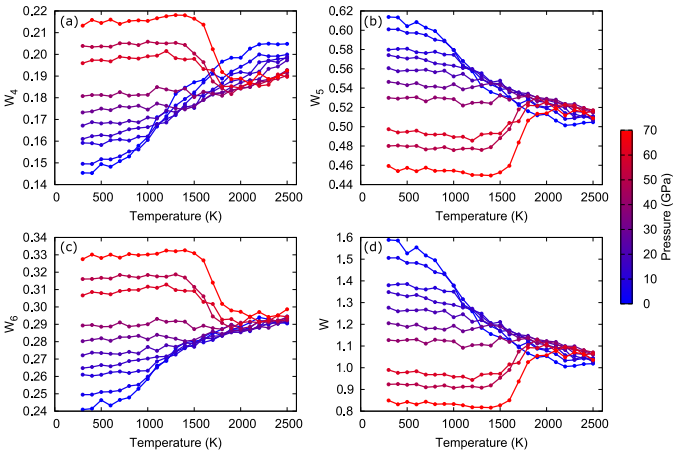

Fig. 6. (a) 4-fold local symmetry parameter, (b) 5-fold local symmetry parameter, (c) 6-fold local symmetry parameter, and (d) $W = \frac{W_5}{W_4 + W_6}$ local symmetry parameter.

Snapshots at different pressures). This last result shows that, for high pressures, the rapidly vitrified alloy can be seen as a mixture of crystal-like regions (yellow-circled zone in Fig. 7) embedded in a glassy matrix (red-colored zones) where the mixed type atoms (in white) form a buffer zone playing the role of interface between the two phases. These crystalline regions embedded in the amorphous zone can exist over scales of 1 to 4 nm (Fig. 7), which is consistent with the correlation length depicted in Fig. 3(b) and in very good agreement with the experimental results suggesting the formation of nanoscale crystals [84,85]. This behavior is also confirmed by the presence of crystal-like atoms, as shown in Fig. 5, which shows that the size and number of the crystal-like zones depend on the applied pressure, which is in the same line of reflection as the work of Zhang et al[45]. As present results, we showed that stress could trigger crystalline regions formation in MGs and demonstrates that by tuning the vitrification conditions, especially the pressure under which the alloy is cooled down, we could design glasses with different crystalline grain size and density depending on the applied pressure.

3.3. Atomic stresses and potential energy

To characterize and understand the atomic structure of glasses under high pressure, we have first used the radial distribution function RDF, which can reflect the statistical average distributions of atoms. However, the physical properties are closely related to the environment of atoms. Consequently, the Voronoi polyhedral analysis has been used. In this method, the relative positions of the nearest neighbor atoms and the topology of atomic connectivity are the most important in determining the behavior of an atom. On the other hand, the physical properties depend not only on the local atomic topology but also on the geometrical distortion of the local polyhedral of nearest neighbor atoms. Atoms in liquids and glasses are not ideally packed as in the closed packed structures, and consequently, the atomic environment of each atom is severely distorted, and then their atomic energies and stresses exhibit non-uniform distributions.

The distribution of energy per atom in $Al_{70}Ni_{15}Co_{15}$ for pressures ranging from 0 to 70 GPa is shown in Fig. 8(a). It should be noted that this distribution at smaller pressures (0, 5 and 10 GPa) is bimodal, as the pressure increases, this latter changes to a unimodal asymmetric distribution with only one main peak. The bimodal distribution is found to be related to a chemical heterogeneity due to different local environments of each atom type in the $Al_{70}Ni_{15}Co_{15}$ MG. This implies that the energy state of these atoms is different and hence make the potential energy distribution bimodal at low pressure. With the increase of the pressure, the atomic potential energy distribution becomes

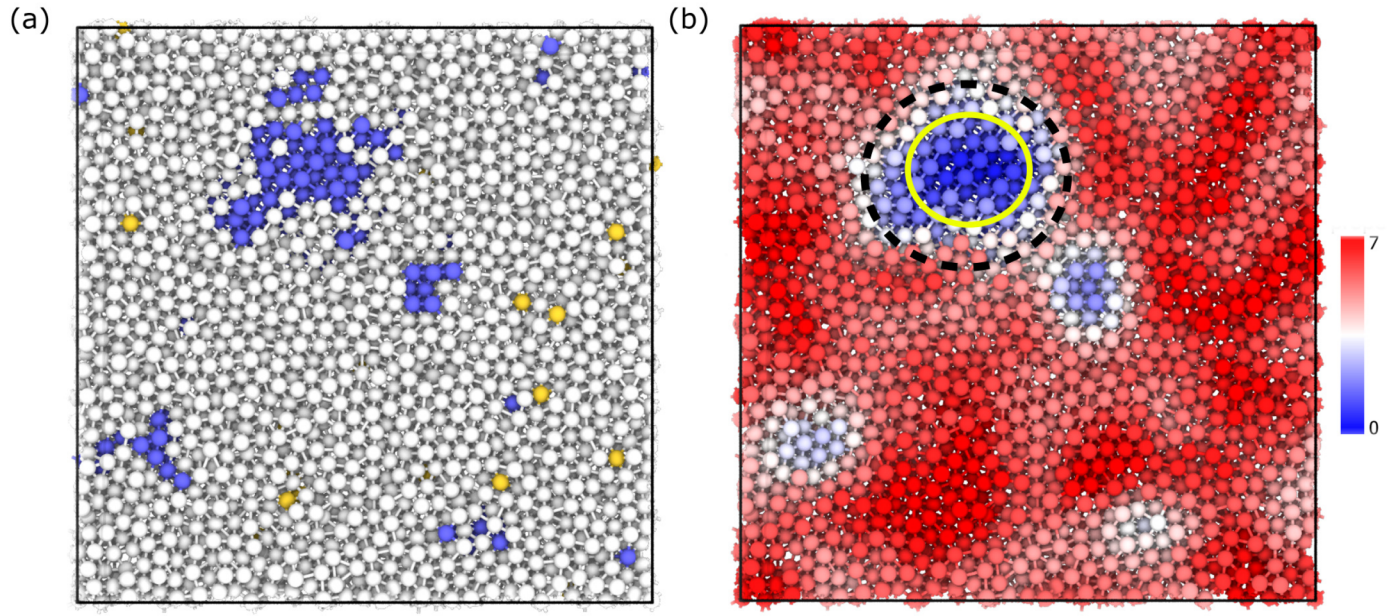

Fig. 7. Slice of width 5 Å from the sample cooled under a pressure of 60 GPa. (a) showing the crystalline structures as identified by the adaptive common neighbors analysis (atoms colors is the same as in Fig. 5), (b) averaged n_5 Voronoi index using a radius of 5 Å . The yellow circle highlights the crystalline region, which shows a very low n_5 Voronoi index the white region, as highlighted by the black dashed circle, indicates a mixed-like region playing the role of an interface between the crystalline region and the amorphous one. The red regions are amorphous. (For interpretation of the references to colour in this figure legend, the reader is referred to the web version of this article.)

unimodal and shifted toward higher values of the potential energy. The decomposition of the total atomic potential energy distribution showed that the values of the potential energy for different atom types are shifted by different rates toward higher values of the potential energy, which results in the disappearance of the two peaks present in the glass cooled under 0 GPa (See Figs. 4 and 5 in the supplementary materials).

In order to describe the local atomic environment, we refer to the concept of atomic-level stresses. First, we would like to emphasize that the stress has a clear physical meaning only when calculated for an ensemble of atoms and poorly defined for individual atoms. Nevertheless, we can use atomic stresses to get some insights on the local state of stress experienced by an atom. We can define the stress as the contribution of each atom to the total virial stress of the system. The stress per atoms was calculated within the framework formulated by Thompson et al. [86] in which, σ_i is defined as follow:

$$\sigma_i = \frac{m_i v_i^2 + \vec{r_i}\cdot\vec{F_i}}{3V_i} \tag{4}$$

where V_i, m_i, v_i, and $\vec{r_i}$ are the volume, mass, velocity, and position of atom i, respectively, and $\vec{F_i}$ is the force applied on atom i by all the other atoms in the system. The volume V_i of each atom is defined as its Voronoi volume. By convention, positive stress refers here to a state of compression, whereas negative stress denotes a state of tension.

In general, the stress is used to characterize the local atomic structure of any system, such as the local structure of liquids, glasses, and crystalline defects, as long as the stress can be attributed to every individual atom. Fig. 8(b) is the distribution of the atomic-level stress in the $Al_{70}Ni_{15}Co_{15}$ alloy for ten different pressures. It can be seen that, with increasing pressure, the atomic level stress distribution shifts towards larger values of stress. Moreover, different atoms have different atomic sizes, when they are mixed under different values of pressures, the average packing scheme, and environment around the atoms is

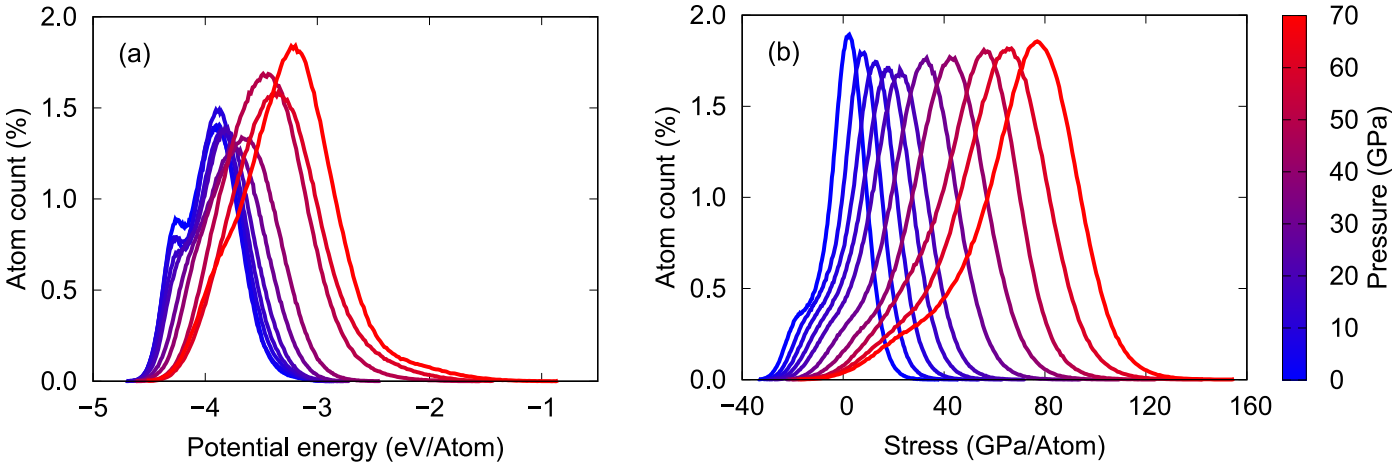

Fig. 8. (a) Potential energy per atom distribution obtained from our MD simulations at 300 K for the studied pressure range. (b) Atomic stress distribution at 300 K and for the studied pressure range in a the $Al_{70}Ni_{15}Co_{15}$ amorphous alloy. Positive and negative stress values denote a state of tension and compression, respectively.

different. However, the average stress on each atom turns out to be almost equal to the absolute value of the overall applied pressure. The stress hinges on the energy associated with it since the thermodynamic stress is defined as the first derivative of energy with respect to the strain tensor. The energy per atom can be evaluated by the changes in the atomic environment of the atoms. This provides how to partition the total energy of the system to each, and every individual atom is crucial for determining the atomic-level stresses. For a glass at 0 GPa, generally, we find atoms under tension and others under compression with a zero mean global value. This is mainly due to the heterogeneous nature of the glasses, which is related to the fluctuation of the local density distribution in the glass. When we apply and external compressive pressure on the glass, we will have more atoms with positive pressure (compression) compared to those under tension and the median of the stress distribution will shift to positive values instead of being zero in the free pressure material. The number of atoms under compression or tension will then strongly depend on the applied pressure.

4. Conclusions

In conclusion, the thermodynamic and structural properties of $Al_{70}Ni_{15}Co_{15}$ metallic glass under high pressure have been investigated by molecular dynamics simulations in the pressure range of 070 GPa. The results from our simulations showed that the glass transition temperature increased with increasing pressure. The obtained atomic structures are then characterized by pair-distribution functions, coordination number, and Voronoi tessellation analysis. It was found that the $Al_{70}Ni_{15}Co_{15}$ metallic glass undergoes structural changes under pressure, which is reflected by a shortening of atomic nearest neighbor distance and an increase of coordination number and crystal-like clusters. This could explain the competition and transformation between local five-fold symmetry and local translational symmetry in local structures during glass formation under pressure. The correlation length as a function of pressure showed that with applying pressure during the cooling process we can induces an increase of the MRO in the glassy structure. The evolution of the heterogeneity of this system with pressure is shown to be related to the formation of nanoscale crystals in the amorphous matrix.

CRediT authorship contribution statement

Achraf Atila: Conceptualization, Methodology, Software, Validation, Formal analysis, Investigation, Data curation, Writing - original draft, Writing - review & editing, Visualization. **Meryem Kbirou:** Conceptualization, Methodology, Validation, Formal analysis, Investigation, Data curation, Writing - original draft, Writing - review & editing. **Said Ouaskit:** Conceptualization, Writing - review & editing, Supervision. **Abdellatif Hasnaoui:** Conceptualization, Writing - review & editing, Visualization, Supervision.

Declaration of Competing Interest

There are no conflicts to declare.

Supplementary material

Supplementary material associated with this article can be found, in the online version, at 10.1016/j.jnoncrysol.2020.120381.

References

[1] Y.-J. Wang, J.-P. Du, S. Shinzato, L.-H. Dai, S. Ogata, A free energy landscape perspective on the nature of collective diffusion in amorphous solids, Acta Mater. 157 (2018) 165–173.

[2] Y.-C. Hu, B.-S. Shang, P.-F. Guan, Y. Yang, H.-Y. Bai, W.-H. Wang, Thermodynamic scaling of glassy dynamics and dynamic heterogeneities in metallic glass-forming liquid, J. Chem. Phys. 145 (10) (2016) 104503, https://doi.org/10.1063/1.4962324.

[3] C. Wang, Z.Z. Yang, T. Ma, Y.T. Sun, Y.Y. Yin, Y. Gong, L. Gu, P. Wen, P.W. Zhu, Y.W. Long, X.H. Yu, C.Q. Jin, W.H. Wang, H.Y. Bai, High stored energy of metallic glasses induced by high pressure, Appl. Phys. Lett. 110 (11) (2017) 111901, https://doi.org/10.1063/1.4978600.

[4] A. Khmich, K. Sbiaai, A. Hasnaoui, Annealing effect on elastic and structural behavior of tantalum monatomic metallic glass, Mater. Chem. Phys. 243 (2020) 122636, https://doi.org/10.1016/j.matchemphys.2020.122636.

[5] A. Khmich, K. Sbiaai, A. Hasnaoui, Structural behavior of tantalum monatomic metallic glass, J. Non. Cryst. Solids 510 (2019) 81–92, https://doi.org/10.1016/j.jnoncrysol.2019.01.024.

[6] C. Ebner, B. Escher, C. Gammer, J. Eckert, S. Pauly, C. Rentenberger, Structural and mechanical characterization of heterogeneities in a CuZr-based bulk metallic glass processed by high pressure torsion, Acta Mater. 160 (2018) 147–157, https://doi.org/10.1016/j.actamat.2018.08.032.

[7] J. Shen, Z. Lu, J. Wang, S. Lan, F. Zhang, A. Hirata, M. Chen, X.-L. Wang, P. Wen, Y.H. Sun, et al., Metallic glacial glass formation by a first-order liquid-liquid transition, J. Phys. Chem. Lett. (2020).

[8] A. Inoue, B. Shen, H. Koshiba, H. Kato, A.R. Yavari, Cobalt-based bulk glassy alloy with ultrahigh strength and soft magnetic properties, Nat. Mater. 2 (10) (2003) 661–663, https://doi.org/10.1038/nmat982.

[9] M.D. Demetriou, M.E. Launey, G. Garrett, J.P. Schramm, D.C. Hofmann, W.L. Johnson, R.O. Ritchie, A damage-tolerant glass, Nat. Mater. 10 (2) (2011) 123–128, https://doi.org/10.1038/nmat2930.

[10] E.D. Zanotto, J.C. Mauro, The glassy state of matter: its definition and ultimate fate, J. Non. Cryst. Solids 471 (2017) 490–495, https://doi.org/10.1016/j.jnoncrysol.2017.05.019.

[11] A. Atila, S. Ouaskit, A. Hasnaoui, Ionic self-diffusion and the glass transition anomaly in aluminosilicates, PCCP 22 (30) (2020) 17205–17212, https://doi.org/10.1039/d0cp02910f.

[12] A. Atila, E.M. Ghardi, S. Ouaskit, A. Hasnaoui, Atomistic insights into the impact of charge balancing cations on the structure and properties of aluminosilicate glasses, Phys. Rev. B 100 (2019) 144109, https://doi.org/10.1103/PhysRevB.100.144109.

[13] A. Atila, E.M. Ghardi, A. Hasnaoui, S. Ouaskit, Alumina effect on the structure and properties of calcium aluminosilicate in the percalcic region: insights from molecular dynamics simulations, J. Non. Cryst. Solids 525 (2019) 119470, https://doi.org/10.1016/j.jnoncrysol.2019.119470.

[14] J. Mo, B. Shen, Y. Wan, Z. Zhou, B. Sun, X. Liang, The effect of thermal history on structure and mechanical properties of Cu64Zr36 metallic glass, J. Non. Cryst. Solids 528 (2020) 119742, https://doi.org/10.1016/j.jnoncrysol.2019.119742.

[15] A. Atila, Atomic structure and modifiers clustering in silicate glasses: effect of modifier cations, arXiv:2007.09247(2020).

[16] E.M. Ghardi, A. Atila, M. Badawi, A. Hasnaoui, S. Ouaskit, Computational insights into the structure of barium titanosilicate glasses, J. Am. Ceram. Soc 102 (11) (2019) 6626–6639, https://doi.org/10.1111/jace.16536.

[17] M. Kbirou, S. Trady, A. Hasnaoui, M. Mazroui, Cooling rate dependence and local structure in aluminum monatomic metallic glass, Philos. Mag. 97 (30) (2017) 2753–2771.

[18] M. Kbirou, M. Mazroui, A. Hasnaoui, Atomic packing and fractal behavior of Al-Co metallic glasses, J. Alloys Compd. 735 (2018) 464–472.

[19] M. Kbirou, A. Hasnaoui, K. Saadouni, M. Badawi, M. Mazroui, Pressure effects on local atomic structure of Ni15Co15Al70 metallic glasses, Comput. Mater. Sci 166 (2019) 20–29.

[20] M. Kbirou, S. Trady, A. Hasnaoui, M. Mazroui, Short and medium-range orders in Co3Al metallic glass, Chem. Phys. 513 (2018) 58–66.

[21] M. Kbirou, S. Trady, A. Hasnaoui, K. Saadouni, et al., Microstructural evolution of Co3Al metallic glass studied by molecular dynamics simulations, Mater. Focus 7 (3) (2018) 346–350.

[22] T.-X. Bui, T.-H. Fang, C.-I. Lee, Effects of flaw shape and size on fracture toughness and destructive mechanism inside Ni15Al70Co15 metallic glass, Comput. Mater. Sci 183 (2020) 109807.

[23] S. Trady, A. Hasnaoui, M. Mazroui, Atomic packing and medium-range order in ni3al metallic glass, J. Non. Cryst. Solids 468 (2017) 27–33.

[24] S. Trady, A. Hasnaoui, M. Mazroui, K. Saadouni, Local atomic structures of single-component metallic glasses, Eur. Phys. J. B 89 (10) (2016) 223.

[25] Y.-C. Hu, P.-F. Guan, Q. Wang, Y. Yang, H.-Y. Bai, W.-H. Wang, Pressure effects on structure and dynamics of metallic glass-forming liquid, J. Chem. Phys. 146 (2) (2017) 024507, https://doi.org/10.1063/1.4973919.

[26] H.B. Lou, Y.K. Fang, Q.S. Zeng, Y.H. Lu, X.D. Wang, Q.P. Cao, K. Yang, X.H. Yu, L. Zheng, Y.D. Zhao, W.S. Chu, T.D. Hu, Z.Y. Wu, R. Ahuja, J.Z. Jiang, Pressure-induced amorphous-to-amorphous configuration change in Ca-Al metallic glasses, Sci. Rep. 2 (1) (2012), https://doi.org/10.1038/srep00376.

[27] Q. Luo, G. Garbarino, B. Sun, D. Fan, Y. Zhang, Z. Wang, Y. Sun, J. Jiao, X. Li, P. Li, N. Mattern, J. Eckert, J. Shen, Hierarchical densification and negative thermal expansion in Ce-based metallic glass under high pressure, Nat. Commun. 6 (1) (2015), https://doi.org/10.1038/ncomms6703.

[28] L. Qi, L. Dong, S. Zhang, M. Ma, Q. Jing, G. Li, R. Liu, Cluster evolution in the rapid cooling process of Cu–Ag melts under high pressure: molecular-dynamics simulation, Comput. Mater. Sci 43 (4) (2008) 732–735, https://doi.org/10.1016/j.commatsci.2008.01.064.

[29] H.W. Sheng, E. Ma, H.Z. Liu, J. Wen, Pressure tunes atomic packing in metallic glass, Appl. Phys. Lett. 88 (17) (2006) 171906, https://doi.org/10.1063/1.2197315.

[30] W.H. Wang, Z.X. Wang, D.Q. Zhao, M.B. Tang, W. Utsumi, X.-L. Wang, High-

pressure suppression of crystallization in the metallic supercooled liquid Zr41Ti14Cu12.5Ni10Be22.5: influence of viscosity, Phys. Rev. B 70 (9) (2004), https://doi.org/10.1103/physrevb.70.092203.
[31] S. Kazanc, Molecular dynamics study of pressure effect on glass formation and the crystallization in liquid CuNi alloy, Comput. Mater. Sci 38 (2) (2006) 405–409.
[32] D. Wen, Y. Deng, J. Liu, Z. Tian, P. Peng, Effect of high pressure on the formation and evolution of clusters during the rapid solidification of zirconium melts, Comput. Mater. Sci 140 (2017) 275–283.
[33] L. Wang, C. Peng, Y. Wang, Y. Zhang, Vitrification and crystallization of metallic liquid under pressures, J. Phys. 18 (32) (2006) 7559.
[34] N. Miyazaki, M. Wakeda, Y.-J. Wang, S. Ogata, Prediction of pressure-promoted thermal rejuvenation in metallic glasses, npj Comput. Mater. 2 (1) (2016) 1–9.
[35] A. Inoue, K. Ohtera, T. Masumoto, New amorphous Al-Y, Al-La And Al-Ce alloys prepared by melt spinning, Jpn. J. Appl. Phys. 27 (5A) (1988) L736.
[36] A.-P. Tsai, A. Inoue, T. Masumoto, Formation of metal-metal type aluminum-based amorphous alloys, Metall. Trans. A 19 (5) (1988) 1369–1371.
[37] A. Inoue, K. Ohtera, K. Kita, T. Masumoto, New amorphous alloys with good ductility in Al-Ce-M (M = Nb, Fe, Co, Ni or Cu) systems, Jpn. J. Appl. Phys. 27 (10A) (1988) L1796.
[38] Y. He, S. Poon, G. Shiflet, Synthesis and properties of metallic glasses that contain aluminum, Science 241 (4873) (1988) 1640–1642.
[39] Y. He, S. Poon, G. Shiflet, Formation and stability of aluminum-based metallic glasses in Al-Fe-Gd alloys, Scr. Metall. 22 (11) (1988) 1813–1816.
[40] X. Shi, X. Wang, Q. Yu, Q. Cao, D. Zhang, J. Zhang, T. Hu, L. Lai, H. Xie, T. Xiao, et al., Structure alterations in Al-Y-based metallic glasses with La and Ni addition, J. Appl. Phys. 119 (11) (2016) 114904.
[41] P. Wang, J.-Q. Wang, H. Li, H. Yang, J. Huo, J. Wang, C. Chang, X. Wang, R.-W. Li, G. Wang, Fast decolorization of azo dyes in both alkaline and acidic solutions by Al-based metallic glasses, J. Alloys Compd. 701 (2017) 759–767.
[42] N. Wu, L. Zuo, J. Wang, E. Ma, Designing aluminum-rich bulk metallic glasses via electronic-structure-guided microalloying, Acta Mater. 108 (2016) 143–151.
[43] J. Qiao, Q. Wang, J. Pelletier, H. Kato, R. Casalini, D. Crespo, E. Pineda, Y. Yao, Y. Yang, Structural heterogeneities and mechanical behavior of amorphous alloys, Prog. Mater. Sci. 104 (2019) 250–329.
[44] F. Zhu, A. Hirata, P. Liu, S. Song, Y. Tian, J. Han, T. Fujita, M. Chen, Correlation between local structure order and spatial heterogeneity in a metallic glass, Phys. Rev. Lett. 119 (21) (2017) 215501.
[45] J. Zhang, G. Liu, J. Sun, Crystallization-aided extraordinary plastic deformation in nanolayered crystalline cu/amorphous Cu-Zr micropillars, Sci. Rep. 3 (1) (2013) 1–6.
[46] Q. An, W.L. Johnson, K. Samwer, S.L. Corona, W.A. Goddard III, Formation of two glass phases in binary Cu-Ag liquid, Acta Mater. (2020).
[47] S. Plimpton, Fast parallel algorithms for short-range molecular dynamics, J. Comput. Phys 117 (1) (1995) 1–19, https://doi.org/10.1006/jcph.1995.1039.
[48] M.S. Daw, M.I. Baskes, Embedded-atom method: derivation and application to impurities, surfaces, and other defects in metals, Phys. Rev. B 29 (12) (1984) 6443.
[49] G.P. Pun, V. Yamakov, Y. Mishin, Interatomic potential for the ternary Ni–Al–Co system and application to atomistic modeling of the B2–L10 martensitic transformation, Modell. Simul. Mater. Sci. Eng. 23 (6) (2015) 065006.
[50] Y. Hu, T.J. Rupert, Atomistic modeling of interfacial segregation and structural transitions in ternary alloys, J. Mater. Sci. 54 (5) (2019) 3975–3993.
[51] Y. Zhou, X. Han, J. Li, Transport properties and abnormal breakdown of the stokes-einstein relation in computer simulated Al72Ni16Co12 metallic melt, J. Non. Cryst. Solids 517 (2019) 83–95.
[52] Y. Li, M. Lv, H. Liang, Local structural arrangement of amorphous Al-Ni-Co alloy during uniaxial tension: a molecular dynamics study, Mater. Trans. 57 (9) (2016) 1505–1508, https://doi.org/10.2320/matertrans.mg201621.
[53] K. Jittisa, C. Wen, W. Hui, D. Amit, F. Meng, P. Gabriela, S.U. D., L. Ze, Y. Rui, D. Wojciech, S.M. D., O.C. S., E. Takeshi, B. Eran, S. Jan, Mechanical glass transition revealed by the fracture toughness of metallic glasses, Nat. Commun. 9 (1) (2018) 3271, https://doi.org/10.1038/s41467-018-05682-8.
[54] J.-P. Guin, Y. Gueguen, Mechanical properties of glass, Springer Handbook of Glass, Springer, 2019, pp. 227–271.
[55] K. Samwer, R. Busch, W. Johnson, Change of compressiblity at the glass transition and Prigogine-Defay ratio in ZrTiCuNiBe alloys, Phys. Rev. Lett. 82 (3) (1999) 580.
[56] I.C. Sanchez, Towards a theory of viscosity for glass-forming liquids, J. Appl. Phys. 45 (10) (1974) 4204–4215.
[57] J. Jiang, W. Roseker, M. Sikorski, Q. Cao, F. Xu, Pressure effect of glass transition temperature in Zr 46.8 Ti 8.2 Cu 7.5 Ni 10 Be 27.5 bulk metallic glass, Appl. Phys. Lett. 84 (11) (2004) 1871–1873.
[58] N.M.A. Krishnan, B. Wang, Y. Le Pape, G. Sant, M. Bauchy, Irradiation-driven amorphous-to-glassy transition in quartz: the crucial role of the medium-range order in crystallization, Phys. Rev. Mater. 1 (2017) 053405, https://doi.org/10.1103/PhysRevMaterials.1.053405.
[59] J. Du, L.R. Corrales, First sharp diffraction peak in silicate glasses: structure and scattering length dependence, Phys. Rev. B 72 (2005) 092201, https://doi.org/10.1103/PhysRevB.72.092201.
[60] S.R. Elliott, Origin of the first sharp diffraction peak in the structure factor of covalent glasses, Phys. Rev. Lett. 67 (1991) 711–714, https://doi.org/10.1103/PhysRevLett.67.711.
[61] P. Scherrer, Bestimmung der inneren struktur und der größe von kolloidteilchen mittels röntgenstrahlen, Kolloidchemie Ein Lehrbuch, Springer, 1912, pp. 387–409.
[62] L. Zhang, F. Sun, X. Hong, J. Wang, G. Liu, L. Kong, H. Yang, X. Liu, Y. Zhao, W. Yang, Pressure-induced polyamorphism by quantitative structure factor and pair distribution function analysis in two ce-based metallic glasses, J. Alloys Compd. 695 (2017) 1180–1184.
[63] D. Ma, A.D. Stoica, X.-L. Wang, Power-law scaling and fractal nature of medium-range order in metallic glasses, Nat. Mater. 8 (1) (2009) 30–34.
[64] F. Li, X. Liu, H. Hou, G. Chen, G. Chen, Structural origin underlying poor glass forming ability of al metallic glass, J. Appl. Phys. 110 (1) (2011) 013519.
[65] D. Han, D. Wei, J. Yang, H.-L. Li, M.-Q. Jiang, Y.-J. Wang, L.-H. Dai, A. Zaccone, Atomistic structural mechanism for the glass transition: entropic contribution, Phys. Rev. B 101 (1) (2020) 014113.
[66] D. Wei, J. Yang, M.-Q. Jiang, L.-H. Dai, Y.-J. Wang, J.C. Dyre, I. Douglass, P. Harrowell, Assessing the utility of structure in amorphous materials, J. Chem. Phys. 150 (11) (2019) 114502.
[67] M. Tahiri, S. Trady, A. Hasnaoui, M. Mazroui, K. Saadouni, K. Sbiaai, Structural properties of Al and TiAl3 metallic glasses–an embedded atom method study, Mod. Phys. Lett. B 30 (16) (2016) 1650170.
[68] M. Tahiri, A. Hasnaoui, K. Sbiaai, Atomic scale investigation of structural properties and glass forming ability of Ti 100- x Al x metallic glasses, Metall. Mater. Trans. A 49 (6) (2018) 2513–2522.
[69] J. Taffs, C.P. Royall, The role of fivefold symmetry in suppressing crystallization, Nat. Commun. 7 (1) (2016) 1–7.
[70] Y. Hu, F. Li, M. Li, H. Bai, W. Wang, Five-fold symmetry as indicator of dynamic arrest in metallic glass-forming liquids, Nat. Commun. 6 (1) (2015) 1–8.
[71] J. Ding, Y.-Q. Cheng, E. Ma, Full icosahedra dominate local order in Cu64Zr34 metallic glass and supercooled liquid, Acta Mater. 69 (2014) 343–354.
[72] Y. Cheng, E. Ma, Atomic-level structure and structure–property relationship in metallic glasses, Prog. Mater. Sci. 56 (4) (2011) 379–473.
[73] D.B. Miracle, A structural model for metallic glasses, Nat. Mater. 3 (10) (2004) 697–702.
[74] H. Sheng, W. Luo, F. Alamgir, J. Bai, E. Ma, Atomic packing and short-to-medium-range order in metallic glasses, Nature 439 (7075) (2006) 419–425.
[75] Y. Shen, T. Kim, A. Gangopadhyay, K. Kelton, Icosahedral order, frustration, and the glass transition: evidence from time-dependent nucleation and supercooled liquid structure studies, Phys. Rev. Lett. 102 (5) (2009) 057801.
[76] D. Miracle, W. Sanders, O. Senkov, The influence of efficient atomic packing on the constitution of metallic glasses, Philos. Mag. 83 (20) (2003) 2409–2428.
[77] D.B. Miracle, E.A. Lord, S. Ranganathan, Candidate atomic cluster configurations in metallic glass structures, Mater. Trans. 47 (7) (2006) 1737–1742.
[78] D. Miracle, O. Senkov, A geometric model for atomic configurations in amorphous Al alloys, J. Non. Cryst. Solids 319 (1–2) (2003) 174–191.
[79] D. Miracle, Efficient local packing in metallic glasses, J. Non. Cryst. Solids 342 (1–3) (2004) 89–96.
[80] D.R. Nelson, Order, frustration, and defects in liquids and glasses, Phys. Rev. B 28 (10) (1983) 5515.
[81] A. Hirata, L. Kang, T. Fujita, B. Klumov, K. Matsue, M. Kotani, A. Yavari, M. Chen, Geometric frustration of icosahedron in metallic glasses, Science 341 (6144) (2013) 376–379.
[82] M. Li, Correlation between local atomic symmetry and mechanical properties in metallic glasses, J. Mater. Sci. Technol. 30 (6) (2014) 551–559.
[83] A. Stukowski, Visualization and analysis of atomistic simulation data with OVITO-the open visualization tool, Model. Simul. Mater. Sci. Eng. 18 (1) (2010) 015012, https://doi.org/10.1088/0965-0393/18/1/015012.
[84] K.B. Kim, J. Das, F. Baier, M.B. Tang, W.H. Wang, J. Eckert, Heterogeneity of a Cu47.5Zr47.5Al5 bulk metallic glass, Appl. Phys. Lett. 88 (5) (2006) 051911, https://doi.org/10.1063/1.2171472.
[85] Y.C. Hu, P.F. Guan, M.Z. Li, C.T. Liu, Y. Yang, H.Y. Bai, W.H. Wang, Unveiling atomic-scale features of inherent heterogeneity in metallic glass by molecular dynamics simulations, Phys. Rev. B 93 (21) (2016), https://doi.org/10.1103/physrevb.93.214202.
[86] A.P. Thompson, S.J. Plimpton, W. Mattson, General formulation of pressure and stress tensor for arbitrary many-body interaction potentials under periodic boundary conditions, J. Chem. Phys. 131 (15) (2009) 154107.